Soil Moisture Retrieval Depth of P- and L-Band Radiometry: Predictions and Observations

Xiaoji Shen, *Graduate Student Member, IEEE*, Jeffrey P. Walker, *Fellow, IEEE*, Nan Ye, Xiaoling Wu, *Member, IEEE*, Nithyapriya Boopathi, *Graduate Student Member, IEEE*, In-Young Yeo, Linlin Zhang, and Liujun Zhu

***Abstract*— The moisture retrieval depth is commonly held to be the approximately top 5 cm at L-band (∼21-cm wavelength/1.41 GHz), which is seen as a limitation for hydrological applications. A widely held view is that this moisture retrieval depth increases with wavelength, ranging approximately from one-tenth to one-fourth of the wavelength. Accordingly, P-band (∼40-cm wavelength/0.75 GHz) is under investigation for soil moisture observation over a deeper layer of soil. However, there is no accepted method for predicting the moisture retrieval depth, and there has been no study to confirm that the actual retrieval depth at P-band is indeed deeper than that achieved at L-band. Consequently, this research has estimated the moisture retrieval depth from theory and compared with empirical evidence from tower-based observations. Model predictions and experimental observations agreed that P-band has the potential to retrieve soil moisture over a deeper layer (∼7 cm) than L-band (∼5 cm) while maintaining the same correlation. However, an alternate interpretation of experimental results is that P-band has a larger correlation with soil moisture (accuracy of retrieval) than L-band but for the same 5-cm moisture retrieval depth. The results also demonstrated the increasing trend of the moisture retrieval depth for increasing wavelength, with the potential to achieving a moisture retrieval depth greater than 10 cm for P-band below 0.5 GHz. Importantly, model predictions showed that moisture retrieval depth was not only dependent on soil moisture content and observation frequency, but also the moisture gradient of the profile.**

***Index Terms*— Coherent model, P-/UHF-band, Polarimetric P-band Multibeam Radiometer (PPMR), soil moisture retrieval/sensing depth.**

Manuscript received June 14, 2020; revised August 13, 2020; accepted September 9, 2020. Date of publication October 7, 2020; date of current version July 22, 2021. This work was supported in part by the Australian Research Council through the Toward P-Band Soil Moisture Sensing from Space Project under Grant DP170102373, in part by Equipment Grants under Grant LE0453434 and Grant LE150100047, in part by the China Scholarship Council (CSC), in part by IITB-Monash Research Academy, and in part by Monash University. *(Corresponding author: Xiaoji Shen.)*

Xiaoji Shen, Jeffrey P. Walker, Nan Ye, Xiaoling Wu, and Liujun Zhu are with the Department of Civil Engineering, Monash University, Clayton, VIC 3800, Australia (e-mail: xiaoji.shen@monash.edu).

Nithyapriya Boopathi is with the Department of Civil Engineering, Monash University, Clayton, VIC 3800, Australia, also with the Center of Studies in Resources Engineering, IIT Bombay, Mumbai 400076, India, and also with the IITB-Monash Research Academy, Mumbai 400076, India.

In-Young Yeo is with the School of Engineering, The University of Newcastle, Callaghan, NSW 2308, Australia.

Linlin Zhang is with the Department of Civil Engineering, Monash University, Clayton, VIC 3800, Australia, and also with the Aerospace Information Research Institute, Chinese Academy of Sciences, Beijing 100101, China.

Digital Object Identifier 10.1109/TGRS.2020.3026384

I. Introduction

SOIL moisture controls various processes in the water, energy, and carbon exchange between the atmosphere and the land surface [1]. Over the past four decades, satellite remote sensing has drawn the community's attention for its potential to provide (near) real-time global soil moisture observations. L-band (∼21-cm wavelength/1.4 GHz) microwave radiometry has been widely accepted as the optimal wavelength for global remote sensing of soil moisture [2] due to: 1) its penetration into the soil and through the vegetation; 2) being a protected band allocated exclusively for radio astronomy use, meaning that it should be clear of radio frequency interference (RFI); and 3) the direct relationship with soil moisture through the soil dielectric constant. Consequently, the two dedicated satellite missions for global soil moisture mapping are at L-band, being European Space Agency (ESA)'s Soil Moisture and Ocean Salinity (SMOS) satellite [3] and National Aeronautics and Space Administration (NASA)'s Soil Moisture Active Passive (SMAP) satellite [4], providing the most widely used soil moisture data set [2], [5], [6]. However, they can only provide moisture information within the top 5-cm layer of soil or less [3], [4] due to the limited moisture sensing depth of L-band, hindering the widespread application of soil moisture products in hydrology, agriculture, and climate research.

Sensing depth is an important concept in microwave remote sensing, indicating the soil depth for which the measured microwave signal is representative. Various terminologies have been used concerning microwave sensing depth, including penetration depth [7], temperature sampling depth [8], and moisture sensing depth [9]. The various terminologies are somewhat confusing and thus need clarification. Generally, the terminology can be categorized into two main classes: one from the aspect of thermal (radiation) and the other from the aspect of reflectivity (dielectric). These are introduced below.

The penetration depth was originally defined as the length over which the energy density associated with an advancing plane wave is reduced to $1/e$ of its initial value [10]. In the early 1970s, penetration depth was estimated by plate experiments, with radiometers observing the response from a metal plate with varying depths of material placed on it [7], [11]. However, the term is somewhat ambiguous because "penetration" implies the wave is penetrating the soil, being the case for

radar rather than radiometry. Later, Wilheit [8] and Njoku *et al.* [9] proposed thermal sampling depth and temperature sensing depth, respectively, which have been used synonymously. The definition in [9] is more specific, with temperature sensing depth expressed as the depth from above which $(1 - 1/e) \approx 63\%$ of the emitted radiation originates. This temperature sensing depth has been understood to increase as wavelength increases [9]. Recently, Lv *et al.* [12] redefined the temperature sensing depth as the depth whereby soil temperature equals the soil effective temperature.

In practice, the moisture sensing (sampling or observation) depth is of primary interest because it indicates the soil thickness whose moisture content can theoretically be retrieved. Njoku *et al.* [9] defined it as the depth below the surface over which moisture (i.e., dielectric constant) determines the reflectivity, and hence the surface emissivity. Accordingly, a common approach for estimating the moisture sensing depth has been to empirically correlate the observed brightness temperature observations with soil moisture measurements averaged over different soil thicknesses [13]–[16].

Moisture sensing depth can be determined only by model estimation rather than by direct measurement, and so it is subject to the retrieval model used. Therefore, use of the term "moisture sensing depth" is considered to be inappropriate as it can be easily misinterpreted as an indicator of the sensing capability of the instrument. More correctly, "moisture retrieval depth" is used hereafter in this article.

In principle, moisture retrieval depth depends on the soil moisture condition and the observation frequency, ranging from approximately one-tenth to one-fourth of the wavelength [8], [17]–[21]. This has inspired the scientific community to explore the potential of P-band (100–30-cm wavelength/ 0.3–1 GHz) in retrieving subsurface ($\sim$10 cm) soil moisture [22]–[24]. However, until now it has not been demonstrated that the moisture retrieval depth at P-band is actually greater than that at L-band due to the lack of radiometer observations at longer wavelengths. Moreover, there is no accepted model for predicting the moisture retrieval depth at different wavelengths.

This article develops a theoretical model for moisture retrieval depth and compares the moisture retrieval depth from P- and L-band radiometry to understand the potential increase at P-band. First, the moisture retrieval depth is theoretically predicted under a range of alternative moisture profiles and sensor wavelengths. Second, the radiometer and soil moisture measurements collected in a tower-based study are empirically correlated with comparing the findings from the theoretical model. Herein, the moisture retrieval depth is defined as the equivalent soil thickness for obtaining an average soil moisture that equates emissivity through the Fresnel equations to the theoretical emissivity from the coherent model.

II. Data

The P-band Radiometer Inferred Soil Moisture (PRISM) project comprises a long-term tower experiment (2017–2020) in Cora Lynn, VIC, Australia [Fig. 1(a)], and airborne campaigns (2019–2021) for undertaking a complete evaluation of P-band radiometer soil moisture remote sensing. A ten-meter-high tower has been installed, carrying two different radiometers [Fig. 1(b)], the Polarimetric P-band Multibeam Radiometer [PPMR, Fig. 1(c)] and the Polarimetric L-band Multibeam Radiometer [PLMR, Fig. 1(d)]. The PPMR and PLMR operate at 0.742–0.752 and 1.400–1.426 GHz, respectively. Moreover, the PPMR has four antenna beams at horizontal (H) and vertical (V) polarizations with 30° beamwidth distributed at angles of $\pm 15°$ and $\pm 45°$ when looking at nadir, while the PLMR has six antenna beams at H- and V-polarizations with 15° beamwidth distributed at angles $\pm 7.5°$, $\pm 21°$, and $\pm 38.5°$ when looking at nadir. Warm and cold point calibrations of the PPMR and PLMR were performed regularly. Warm point calibrations were undertaken weekly by placing PPMR/PLMR over a blackbody chamber containing microwave absorber and 16 temperature sensors. Cold point calibrations were performed every midnight according to the tower schedule by facing the PPMR and PLMR to the sky. The calibration accuracy for both PPMR and PLMR is less than 1.5 K. Please note that the use of "P-band" and "L-band" hereafter specifically refers to the frequencies at which PPMR and PLMR are operating unless otherwise specified.

The temporal evolution of soil moisture was monitored by a station [Fig. 1(e)] having hydra-probes inserted into the soil from the surface down to 25 cm, with measurements covering each 5-cm increment. The top probe was installed vertically from the surface while the others were installed horizontally, with the probe pins being 5 cm long. These probes continuously measured soil temperature and moisture at a 20-min sampling step. Particle size analysis on soil samples collected over the field found the soil to be a silt loam consisting of 18.0% clay, 10.9% sand, and 71.1% silt. The soil bulk density of the surface soil layer in this site is 0.87 g/cm^3. Refer [24] and [25] for more details for specifications of the instruments and the experimental setup.

The tower automatically rotated the mast on a schedule such that PPMR and PLMR alternatively observed the same soil, with P- and L-band observations separated by no more than half an hour. The instrument was tilted to produce a range of incidence angles from 30° to 60°, with the footprints of PPMR and PLMR at 30° and 60° incidence angle shown in Fig. 1(a). The spatial homogeneity of the soil moisture at this site was ensured by regular spatial measurements of surface soil moisture ($\sim$5 cm) using the Monash University Hydraprobe Data Acquisition System (HDAS) [26].

Data at 30° incidence angle from May 9, 2019, to June 12, 2019, an observation period during which the field was maintained as flat bare ground with dynamic moisture conditions, have been used for the empirical correlation analysis in this article. To minimize the presence of weeds, the experiment site was freshly plowed on May 7, 2019.

III. Method

A. Radiative Transfer Theory

Radiometers measure the intensity of thermal emission from soil in the form of a brightness temperature (TB_P), where subscript P denotes either H- or V-polarization. For an

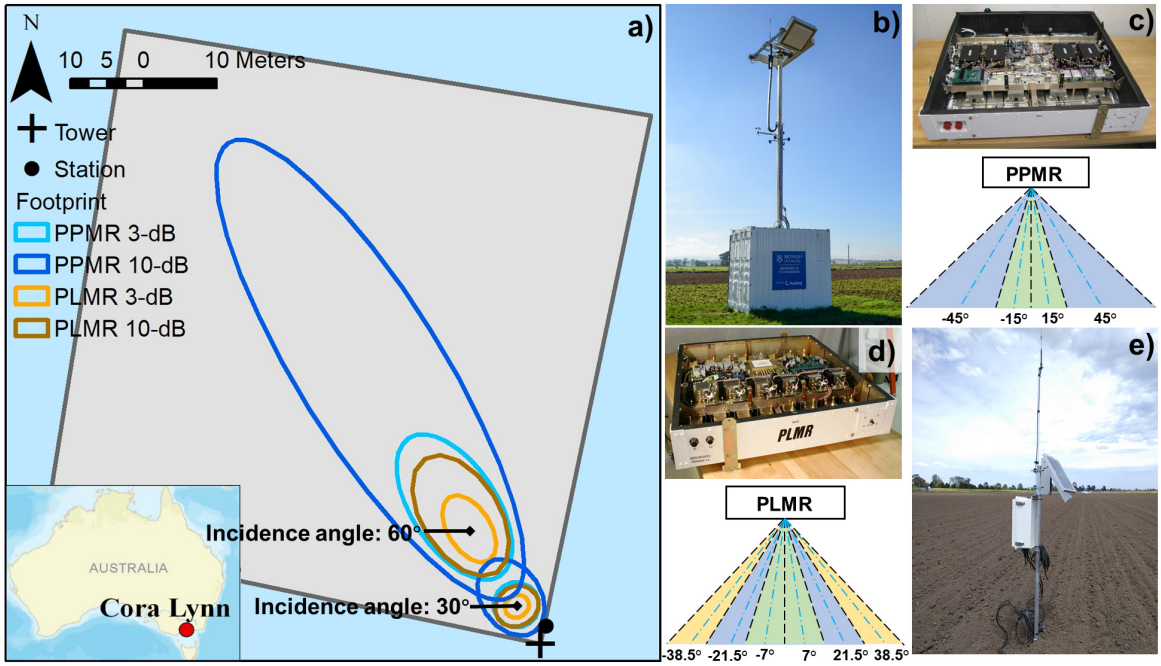

Fig. 1. (a) Map of the tower-based experiment site at Cora Lynn, Melbourne, Australia. (b) Tower carrying PPMR and PLMR. (c) PPMR with four antenna beams. (d) PLMR with six antenna beams. (e) Monitoring station.

ideal bare soil medium with a smooth surface and uniform moisture (SM) and temperature (T) profile, the well-known radiative transfer approximation, also known as the zero-order noncoherent model, can be used to estimate the emissivity (e_P) from [20]

$$\mathrm{TB}_P = e_P T. \tag{1}$$

Kirchoff's reciprocity theorem relates emissivity to soil Fresnel reflectivity (Γ_P^*) through

$$e_P = 1 - \Gamma_P^* \tag{2}$$

where Γ_P^* can be computed using the Fresnel equation as a function of the relative soil dielectric constant ε_r ($\varepsilon_r = \varepsilon_r' - i \cdot \varepsilon_r''$) including real ($'$) and imaginary ($''$) parts, and the incidence (observation) angle (θ) from nadir, expressed as

$$\Gamma_H^* = \left| \frac{\cos(\theta) - \sqrt{\varepsilon_r - \sin^2(\theta)}}{\cos(\theta) + \sqrt{\varepsilon_r - \sin^2(\theta)}} \right|^2 \tag{3}$$

$$\Gamma_V^* = \left| \frac{\varepsilon_r \cdot cos(\theta) - \sqrt{\varepsilon_r - \sin^2(\theta)}}{\varepsilon_r \cdot \cos(\theta) + \sqrt{\varepsilon_r - \sin^2(\theta)}} \right|^2. \tag{4}$$

Finally, the soil dielectric constant can be related to the soil moisture by a dielectric mixing model such as [27]–[29].

For real soils, moisture and temperature vary vertically due to solar radiation, precipitation, infiltration, and gravity, so are by no means uniform. Stratified coherent models are able to simulate the TB for a soil medium with nonuniform temperature and moisture, expressed as [19], [30]

$$\mathrm{TB}_P = \int_0^\infty T(z) f_P(z) dz \tag{5}$$

where $T(z)$ is the soil temperature at depth z, and $f_P(z)$ is the fractional absorption which is calculated from solution of a differential equation with a flux conservation boundary condition at the air/soil interface, such that

$$f_H(z) = \int_0^\infty \frac{k}{\cos(\theta)} \varepsilon_r''(z) |\psi(z)|^2 dz \tag{6}$$

$$f_V(z) = \int_0^\infty \frac{1}{k\cos(\theta)} \varepsilon_r''(z) \cdot \left(\left| \frac{1}{\varepsilon_r(z)} \frac{d\phi(z)}{dz} \right|^2 + \left| \frac{k_x \phi(z)}{\varepsilon_r(z)} \right|^2 \right) dz \tag{7}$$

where k is the free space wavenumber ($2\pi/\lambda$), $k_x = k\sin(\theta)$, and the functions $\psi(z)$ and $\phi(z)$ are determined from [30]

$$\frac{d^2\psi(z)}{dz^2} + \left[\varepsilon_r(z)k^2 - k_x^2\right]\psi(z) = 0 \tag{8}$$

$$\varepsilon_r(z) \frac{d}{dz} \left(\frac{1}{\varepsilon_r(z)} \frac{d\phi(z)}{dz} \right) + \left[\varepsilon_r(z)k^2 - k_x^2\right]\phi(z) = 0. \tag{9}$$

Refer to Njoku [31] for more details on the mathematical derivation of the coherent model.

In order to apply the radiative transfer approximation to soils with nonuniform temperature, the so-called effective temperature (T_{eff}) was proposed to substitute the physical temperature (T) in (1). Accordingly, T_{eff} is defined as the equivalent temperature for an ideal isothermal soil medium having the same microwave response as that for the natural soil, expressed as [19]

$$T_{\mathrm{eff}} = \frac{\int_0^\infty T(z) f(z) dz}{\int_0^\infty f(z) dz}. \tag{10}$$

Subsequently, T_{eff} has been simplified to a parameter associated with observation frequency, surface and deep temperature

of the soil [32]. Thus, with known TB_P and $T = T_{\text{eff}}$, e_P can be obtained from (1). However, the question of what representative depth of soil over which the emissivity (i.e., dielectric constant and thus moisture) is estimated remains.

B. Moisture Retrieval Depth Model

To quantify the above-mentioned representative depth, the moisture retrieval depth (δ_m) is defined as the equivalent soil thickness $[0, z]$ for obtaining an average soil moisture that equates the emissivity through the Fresnel equations (hereafter referred to as the Fresnel emissivity) to the theoretical emissivity from the coherent model (hereafter referred to as the coherent emissivity). The mathematical explanations are as follows.

Equating (1) and (5) and substituting (10), one obtains

$$e(\text{SM}(0-\delta_m)) = \int_0^\infty f(z)dz \tag{11}$$

where $\text{SM}(0-\delta_m)$ is the soil moisture averaged over 0–δ_m, $e(\text{SM}(0-\delta_m))$ denotes the Fresnel emissivity determined by $\text{SM}(0-\delta_m)$, and $\int_0^\infty f(z)dz$ is the coherent emissivity. Equation (11) can therefore be used to determine the soil thickness whose averaged soil moisture produces a Fresnel emissivity (term on the left-hand side) that equals the coherent emissivity (term on the right-hand side).

To account for the roughness effects of a natural soil medium, the widely used roughness model [15], [33] was adopted, such that

$$e_R = (e^*-1)\exp\left(-H_R\cos^2(\theta)\right) \tag{12}$$

for low frequencies, i.e., P- and L-bands, where e^* and e_R are the Fresnel/coherent emissivity before and after accounting for the roughness effects, respectively, and H_R is a roughness parameter that characterizes the intensity of the roughness effects. Substituting the Fresnel and coherent emissivity in (11) with e_R demonstrates that roughness has no impact on moisture retrieval depth according to this model. Consequently, roughness effects were not considered in this article.

C. Moisture Retrieval Depth Prediction

In this article, (11) was used to predict the moisture retrieval depth for a range of typical soil moisture profiles (Fig. 2) using the soil properties of Cora Lynn. Dielectric constant was estimated from soil moisture by the Mironov model [34], because it accounts for the interfacial (Maxwell–Wagner) relaxation of water in the soil at P-band [34], differing from the dielectric model developed dedicatedly for SMOS at L-band [29]. Inputs to the Mironov model include soil moisture, frequency, bulk density, and clay content of the soil. It neglects the insignificant dependence of temperature on the dielectric constant by assuming a constant temperature of 20 °C. In summary, the required inputs of this moisture retrieval depth model are therefore the soil moisture profile, soil properties (clay content and bulk density), observation frequency, and incidence angle. The incidence angle used was 30° for consistency with the TB observations used in this article.

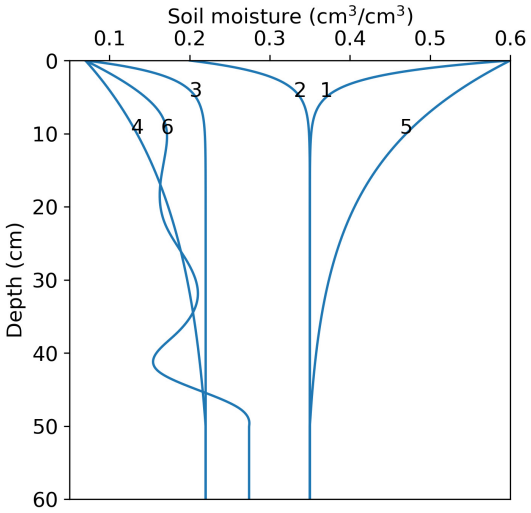

Fig. 2. Simulated typical soil moisture profiles with constant moisture assumed below 50 cm.

TABLE I
PARAMETERS CHARACTERIZING THE MOISTURE PROFILES PLOTTED IN FIG. 2

Profile	SM_s (cm^3/cm^3)	ΔSM (cm^3/cm^3)	β (cm^{-1})	d (cm)	Moisture gradient over 0-10 cm layer (cm^{-1})	Moisture gradient over 10-20 cm layer (cm^{-1})
1	60	-25	0.5	50	0.025	0
2	20	15	0.5	50	0.015	0
3	7	15	0.5	50	0.015	0
4	7	15	0.05	50	0.006	0.004
5	60	-25	0.07	50	0.013	0.006
6	-	-	-	-	0.010	0.001

Six typical soil moisture profiles $\text{SM}(z)$ (Fig. 2) were used for the estimation of the moisture retrieval depth assuming constant moisture below 50 cm. Profiles 1–5 were simulated using the functions from [30] being

$$\text{SM}(z) = \text{SM}_s + \Delta\text{SM}\frac{e^{-\beta z}-1}{e^{-\beta d}-1} \quad 0 \le z \le d \tag{13}$$

$$\text{SM}(z) = \text{SM}(d) \quad z \ge d \tag{14}$$

and the parameters listed in Table I, where SM_s is the moisture content at the soil surface, ΔSM is the increment of moisture between the surface and depth d below the surface, beyond which the moisture content is assumed to be constant, and β determines the moisture gradient of the profile.

Profiles 1 and 5 may both occur during rain but with different rainfall amounts, duration, and intensity. Profiles 2–4 simulate drying profiles. Profiles 2 and 3 have the same moisture gradient near the surface but different profile moisture, while profile 4 has a smaller surface moisture gradient. Differing from profiles 1–5, profile 6 represents the actual moisture profile observed at the Cora Lynn tower site, generated by interpolating the soil moisture measurements at different depths from the station. Profile depth and layer thickness of all six profiles were assumed to be 10 m

(i.e., $z < 10$ m) and 0.1 mm, respectively, to avoid any possible boundary or numerical approximation artifacts.

D. Moisture Retrieval Depth Observation

For empirical estimation of moisture retrieval depth using the tower observations, the microwave polarization difference index (MPDI) [35] expressed as

$$\text{MPDI} = \frac{\text{TB}_V - \text{TB}_H}{\text{TB}_V + \text{TB}_H} \tag{15}$$

was correlated with the averaged soil moisture measurements over different soil thicknesses. MPDI was used instead of TB to exclude the impact of diurnal or day-to-day variations in soil temperature on brightness temperature, and thus be more highly related to the dielectric properties (i.e., moisture) of the soil [36].

IV. Results and Discussion

A. Predicted Moisture Retrieval Depth

Prior to estimation of the moisture retrieval depth, the complex relative dielectric constant and emissivity were compared for P- and L-bands in Fig. 3. It can be seen that the real components of the dielectric constant are basically the same across soil moisture at P- and L-bands whereas P-band has a slightly larger imaginary component than L-band, in line with [37] and [38]. The emissivity was predicted by both the Fresnel and coherent model and found to be the same for the scenario of an assumed uniform moisture and temperature profile. The slight difference in dielectric constant resulted in a small unapparent offset in emissivity at P- and L-bands, particularly when soil moisture is less than 0.3 cm^3/cm^3.

Fig. 4 depicts the estimated coherent and Fresnel emissivity across soil thickness corresponding to the moisture profiles 1–6 of Fig. 2 at 30° incidence angle at H-polarization. The impact of incidence angle and polarization on moisture retrieval depth was also investigated (results not shown), with only minor variations found. This is in line with [8], which explained that the direction of propagation through the medium remains closely normal to the interface even for oblique incidence as a result of Snell's law. The impact of soil texture on moisture retrieval depth was also tested by assuming a clay content of 50% instead of 18% (results not shown) with a difference of not more than 1 cm between the two results.

By definition, the simulated coherent emissivity for each profile is a single value and thus plotted in Fig. 4 as the solid horizontal line. The Fresnel emissivity was calculated using the averaged soil moisture over an increasing soil thickness, shown as the dashed curve. The moisture retrieval depth for P- and L-bands is thus indicated by the intersection of the two models. However, this theoretical retrieval depth is subject to uncertainties.

To account for uncertainties, the moisture retrieval depth was calculated as the vertical dotted lines shown in Fig. 4. One major uncertainty source is considered to be the dielectric model because most dielectric models are semiempirical. A comprehensive evaluation of nine commonly used dielectric models by Park *et al.* [39] found an average median

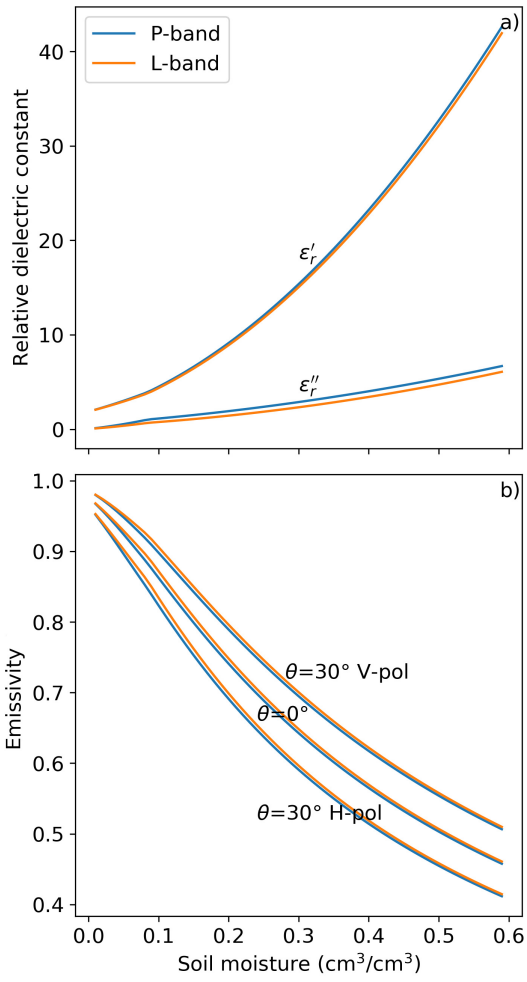

Fig. 3. Comparison of P- and L-bands (a) relative dielectric constant and (b) emissivity, across soil moisture. The dielectric constant was predicted by the Mironov model [34] for 20 °C soil temperature, 18.0% clay, 10.9% sand, 71.1% silt, and 0.87-g/cm^3 bulk density.

absolute bias of around 0.03 cm^3/cm^3 when compared with measurements. Accordingly, the potential bias in emissivity can be estimated depending on the soil moisture and frequency. Moreover, in a practical sense, soil is a continuous medium and thus high correlation exists between the soil moisture of neighboring layers, potentially enlarging the moisture retrieval depth further. Therefore, the moisture retrieval depth in this article was increased to the point where the difference between the Fresnel and coherent emissivity was equal to the above-mentioned bias in emissivity.

The calculated moisture retrieval depths in Fig. 4 ranged within 0.8–10.5 and 0.6–8.4 cm for P- and L-band at 30° incidence angle, respectively. Overall, larger moisture retrieval depth at P-band than L-band can be observed for all profiles, especially profiles 2, 3, 4, and 6. However, P- and L-bands did not show much difference for profiles 1 and 5 due to the extremely high surface soil moisture. Fig. 5 demonstrates that, overall, the moisture retrieval depth increased with wavelength, particularly when the frequency dropped below 1 GHz, though minimally for profiles 1 and 5 due to the extremely high surface soil moisture. The moisture retrieval depth of

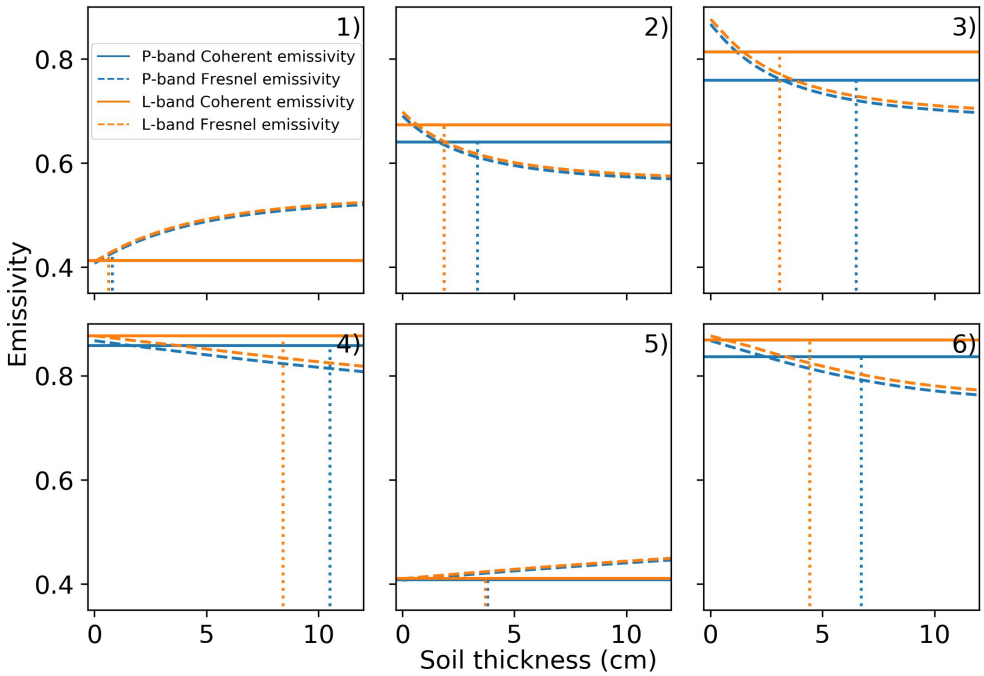

Fig. 4. Coherent and Fresnel emissivity at 30° incidence angle and H-polarization across soil thickness and moisture retrieval depth indicated by vertical dotted lines. Subplots 1–6 correspond to soil moisture profiles 1–6. In subplots 1 and 5, P- and L-bands are very close to being overlapped.

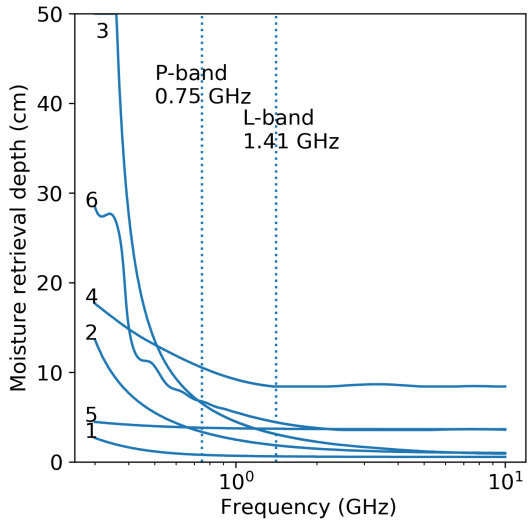

Fig. 5. Moisture retrieval depth at 30° incidence angle and H-polarization against frequency from 0.3 to 10 GHz, corresponding to soil moisture profiles 1–6.

profile 6 has some "waves" across frequency due to the irregular fluctuation of soil moisture with depth.

Fig. 5 also shows that the soil moisture, especially the surface soil moisture relative to the profile soil moisture, has the primary impact on determining the moisture retrieval depth, e.g., a sequence of moisture retrieval depth from large to small is profiles 3, 2, and 1, corresponding to the surface soil moisture from low to high. This frequency and moisture dependence of moisture retrieval depth has also been observed by previous empirical studies at L-band [8], [13]. However, this cannot explain why profile 5 achieved a larger moisture retrieval depth than profile 1, even though it had a higher surface and subsurface moisture. It is therefore reasonable to infer that the moisture gradient is another primary factor that dominates moisture retrieval depth.

It is hypothesized that the lower surface moisture gradient in the 0–10-cm layer of 0.013 cm^{-1} contributed to the deeper moisture retrieval depth of profile 5, compared to profile 1 whose surface moisture gradient was 0.025 cm^{-1} (Table I), because a lower gradient usually means a higher correlation between the moisture of neighboring soil layers. Moreover, it was observed that the moisture gradient in the 10–20-cm layer affected the moisture retrieval depth. Profiles 2 and 3 have a large surface moisture gradient of 0.015 cm^{-1} but are then uniform below 10 cm. This explains why in Fig. 5 for decreasing frequency the moisture retrieval depth increased slowly at first and then quickly below 0.5 GHz for these profiles. For the continuously changing profiles 4 and 5, the moisture retrieval depth did not change much over frequency. Therefore, P-band tended to have a substantially larger moisture retrieval depth than L-band only if the moisture profile was steep at the surface and then uniform for deeper depths, with dry-to-intermediate soil moisture (e.g., profile 3). Otherwise, P- and L-bands had a similar moisture retrieval depth (e.g., profiles 4 and 5).

B. Observed Moisture Retrieval Depth

Fig. 6 shows the data collected over the flat bare soil study site at an incidence angle of 30° from May 9, 2019, to June 12, 2019. Only the TB data collected at approximately 6 A.M. were plotted and used here, to minimize uncertainties from a nonuniform soil temperature profile, and any diurnal temperature variations. The data gaps in the TB, shown by

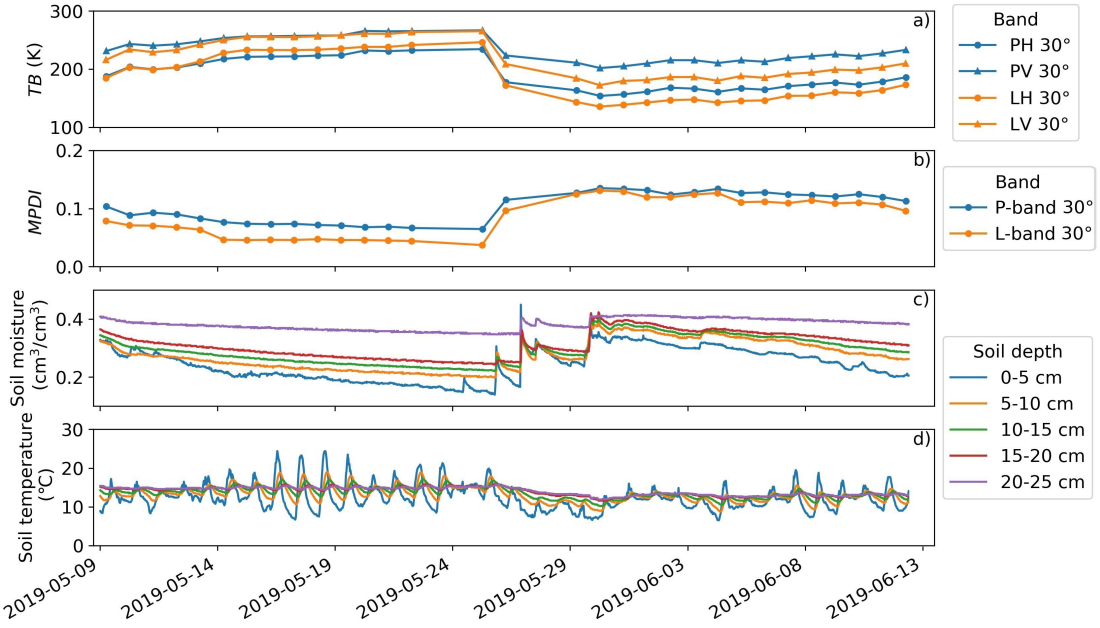

Fig. 6. Data collected over bare and flat soil, including (a) TB observations, (b) calculated MPDI from TB, (c) station time series soil moisture, and (d) soil temperature.

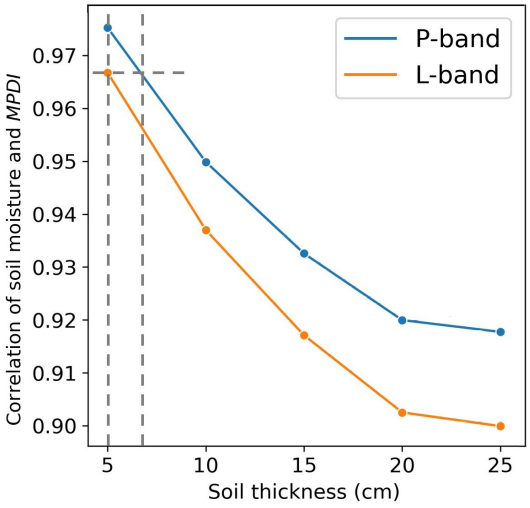

Fig. 7. Correlation of MPDI against soil moisture averaged over different soil thicknesses for bare soil observations from May 9, 2019, to June 12, 2019. The dashed lines show that P-band has larger soil thickness than L-band for the same correlation, or larger correlation for the same soil thickness.

irregular spacing of data points, resulted from the tower being lowered due to high wind.

The MPDI was calculated from the TB measurements using (15) and correlated with the soil moisture measurements averaged over different soil thicknesses. Fig. 7 shows the correlation of MPDI against soil moisture for P- and L-bands. It can be observed that the correlation was highest for the 0–5 cm thickness and decreased with increasing soil thickness. This result can be interpreted in one of two ways: 1) for the same moisture retrieval depth (∼5 cm) a greater correlation (accuracy of retrieval) can be achieved at P-band than at L-band or 2) a larger moisture retrieval depth can be achieved at P-band (∼7 cm) than at L-band (∼5 cm) for the same correlation (accuracy of retrieval), confirming the prediction result for profile 6. Importantly, these empirical results are limited to the specific moisture conditions, soil properties, and incidence angle used in the Cora Lynn site.

V. Conclusion

This article compared the moisture retrieval depth of P- and L-band radiometry to demonstrate the potential of P-band for a future satellite mission with deeper subsurface moisture sensing. Theoretical simulations were first performed to predict the moisture retrieval depth with simulated soil profiles by equating the coherent and Fresnel emissivity. Empirical correlation analysis was then applied to the MPDI from observed brightness temperature and soil moisture measurements collected in a tower-based experiment over a flat bare soil.

A higher correlation between soil moisture and MPDI was found at P-band than L-band for the same moisture retrieval depth, suggesting that P-band can either retrieve soil moisture over the same moisture retrieval depth as L-band (∼5 cm) but with higher accuracy, or that a larger moisture retrieval depth (∼7 cm) can be achieved while maintaining the same accuracy. These empirical results agreed with predictions. Moreover, predictions showed that the moisture retrieval depth increased with wavelength such that P-band can potentially provide soil moisture retrievals for a depth greater than 10 cm when using a frequency lower than 0.5 GHz. However, it was found that the moisture retrieval depth achieved was dependent on the moisture gradient of the profile in addition to the soil moisture content and observation frequency.

Acknowledgment

The authors wish to thank Pascal Mater and Kiri Mason for their help with maintenance of the experimental site.

Thanks also go to the two anonymous reviewers for their helpful comments and suggestions.

REFERENCES

[1] S. I. Seneviratne *et al.*, "Investigating soil moisture-climate interactions in a changing climate: A review," *Earth-Sci. Rev.*, vol. 99, nos. 3–4, pp. 125–161, 2010.

[2] J. P. Wigneron *et al.*, "Modelling the passive microwave signature from land surfaces: A review of recent results and application to the L-band SMOS & SMAP soil moisture retrieval algorithms," *Remote Sens. Environ.*, vol. 192, pp. 238–262, Apr. 2017.

[3] Y. H. Kerr *et al.*, "The SMOS mission: New tool for monitoring key elements of the global water cycle," *Proc. IEEE*, vol. 98, no. 5, pp. 666–687, May 2010.

[4] D. Entekhabi *et al.*, "The soil moisture active passive (SMAP) mission," *Proc. IEEE*, vol. 98, no. 5, pp. 704–716, May 2010.

[5] Y. Gao *et al.*, "Evaluation of the Tau–Omega model for passive microwave soil moisture retrieval using SMAPEx datasets," *IEEE J. Sel. Topics Appl. Earth Observ. Remote Sens.*, vol. 11, no. 3, pp. 888–895, Mar. 2018.

[6] X. Li *et al.*, "Compared performances of SMOS-IC soil moisture and vegetation optical depth retrievals based on tau-omega and two-stream microwave emission models," *Remote Sens. Environ.*, vol. 236, Jan. 2020, Art. no. 111502.

[7] J. Conel, "Microwave emission from granular silicates-determination of the absorption coefficient from plate measurements and the effects of scattering," Jet Propuls. Lab., California Inst. Technol., Pasadena, CA, USA, Tech. Memorandum 33-485, 1970.

[8] T. T. Wilheit, "Radiative transfer in a plane stratified dielectric," *IEEE Trans. Geosci. Electron.*, vol. 16, no. 2, pp. 138–143, Apr. 1978.

[9] E. G. Njoku, J. Schiedge, and A. B. Kahle, *Joint Microwave and Infrared Studies for Soil Moisture Determination*. La Cañada Flintridge, CA, USA: Jet Propulsion Laboratory, 1980.

[10] M. Born and E. Wolf, *Principles of Optics. Second (Revised) Edition*, vol. 12. New York, NY, USA: Macmillan Co., 1964, p. 124.

[11] J. C. Blinn and J. G. Quade, "Microwave properties of geological materials: Studies of penetration depth and moisture effects," presented at the 4th Annu. Earth Resour. Program Rev., NASA, Lyndon B. Johnson Space Center, Houston, TX, USA, Jan. 1972.

[12] S. Lv, Y. Zeng, Z. Su, and J. Wen, "A closed-form expression of soil temperature sensing depth at L-band," *IEEE Trans. Geosci. Remote Sens.*, vol. 57, no. 7, pp. 4889–4897, Jul. 2019.

[13] M. J. Escorihuela, A. Chanzy, J. P. Wigneron, and Y. H. Kerr, "Effective soil moisture sampling depth of L-band radiometry: A case study," *Remote Sens. Environ.*, vol. 114, no. 5, pp. 995–1001, May 2010.

[14] D. Zheng *et al.*, "Sampling depth of L-band radiometer measurements of soil moisture and freeze-thaw dynamics on the tibetan plateau," *Remote Sens. Environ.*, vol. 226, pp. 16–25, Jun. 2019.

[15] J. Wang and B. Choudhury, "Remote sensing of soil moisture content, over bare field at 1.4 GHz frequency," *J. Geophys. Res. Oceans*, vol. 86, no. C6, pp. 5277–5282, 1981.

[16] S. Paloscia, P. Pampaloni, L. Chiarantini, P. Coppo, S. Gagliani, and G. Luzi, "Multifrequency passive microwave remote sensing of soil moisture and roughness," *Int. J. Remote Sens.*, vol. 14, no. 3, pp. 467–483, Feb. 1993.

[17] R. W. Newton, Q. R. Black, S. Makanvand, A. J. Blanchard, and B. R. Jean, "Soil moisture information and thermal microwave emission," *IEEE Trans. Geosci. Remote Sens.*, vol. GE-20, no. 3, pp. 275–281, Jul. 1982.

[18] S. Raju, A. Chanzy, J.-P. Wigneron, J.-C. Calvet, Y. Kerr, and L. Laguerre, "Soil moisture and temperature profile effects on microwave emission at low frequencies," *Remote Sens. Environ.*, vol. 54, no. 2, pp. 85–97, Nov. 1995.

[19] T. J. Schmugge and B. J. Choudhury, "A comparison of radiative transfer models for predicting the microwave emission from soils," *Radio Sci.*, vol. 16, no. 5, pp. 927–938, Sep. 1981.

[20] F. T. Ulaby, R. K. Moore, and A. K. Fung, *Microwave Remote Sensing: Active and Passive.: From Theory to Applications*, vol. 22, no. 5. Norwood, MA, USA: Artech House, 1986, pp. 1223–1227.

[21] R. W. Newton, J. L. Heilman, and C. H. M. Van Bavel, "Integrating passive microwave measurements with a soil moisture/heat flow model," *Agricult. Water Manage.*, vol. 7, nos. 1–3, pp. 379–389, Sep. 1983.

[22] A. Tabatabaeenejad, M. Burgin, X. Duan, and M. Moghaddam, "P-band radar retrieval of subsurface soil moisture profile as a second-order polynomial: First AirMOSS results," *IEEE Trans. Geosci. Remote Sens.*, vol. 53, no. 2, pp. 645–658, Feb. 2015.

[23] S. Yueh, R. Shah, X. Xu, K. Elder, and B. Starr, "Experimental demonstration of soil moisture remote sensing using P-band satellite signals of opportunity," *IEEE Geosci. Remote Sens. Lett.*, vol. 17, no. 2, pp. 207–211, Feb. 2020.

[24] N. Ye *et al.*, "Toward P-band passive microwave sensing of soil moisture," *IEEE Geosci. Remote Sens. Lett.*, to be published, Mar. 16, 2020, doi: 10.1109/LGRS.2020.2976204.

[25] N. Boopathi *et al.*, "Towards soil moisture retrieval using tower-based P-band radiometer observations," in *Proc. IEEE Int. Geosci. Remote Sens. Symp. IGARSS*, Jul. 2018, pp. 1407–1410.

[26] O. Merlin, J. P. Walker, R. Panciera, R. Young, J. D. Kalma, and E. J. Kim, "Soil moisture measurement in heterogeneous terrain," presented at the Modsim Int. Congr. Modeling Simulation Land Water Environ. Manage. Integr. Syst. Sustainability, Dec. 2007.

[27] N. R. Peplinski, F. T. Ulaby, and M. C. Dobson, "Dielectric properties of soils in the 0.3-1.3-GHz range," *IEEE Trans. Geosci. Remote Sens.*, vol. 33, no. 3, pp. 803–807, May 1995.

[28] M. Dobson, F. Ulaby, M. Hallikainen, and M. El-rayes, "Microwave dielectric behavior of wet soil—Part II: Dielectric mixing models," *IEEE Trans. Geosci. Remote Sens.*, vol. GE-23, no. 1, pp. 35–46, Jan. 1985.

[29] V. Mironov, Y. Kerr, J.-P. Wigneron, L. Kosolapova, and F. Demontoux, "Temperature- and texture-dependent dielectric model for moist soils at 1.4 GHz," *IEEE Geosci. Remote Sens. Lett.*, vol. 10, no. 3, pp. 419–423, May 2013.

[30] E. G. Njoku and J.-A. Kong, "Theory for passive microwave remote sensing of near-surface soil moisture," *J. Geophys. Res.*, vol. 82, no. 20, pp. 3108–3118, Jul. 1977.

[31] E. G. Njoku, *Microwave Remote Sensing of Near-Surface Moisture and Temperature Profiles*. Cambridge, MA, USA: Massachusetts Institute of Technology, 1976.

[32] B. J. Choudhury, T. J. Schmugge, and T. Mo, "A parameterization of effective soil temperature for microwave emission," *J. Geophys. Res. Oceans*, vol. 87, no. C2, pp. 1301–1304, Feb. 1982.

[33] H. Lawrence, J.-P. Wigneron, F. Demontoux, A. Mialon, and Y. H. Kerr, "Evaluating the semiempirical $H-Q$ model used to calculate the L-band emissivity of a rough bare soil," *IEEE Trans. Geosci. Remote Sens.*, vol. 51, no. 7, pp. 4075–4084, Jul. 2013.

[34] V. L. Mironov, P. P. Bobrov, and S. V. Fomin, "Multirelaxation generalized refractive mixing dielectric model of moist soils," *IEEE Geosci. Remote Sens. Lett.*, vol. 10, no. 3, pp. 603–606, May 2013.

[35] F. Becker and B. J. Choudhury, "Relative sensitivity of normalized difference vegetation index (NDVI) and microwave polarization difference index (MPDI) for vegetation and desertification monitoring," *Remote Sens. Environ.*, vol. 24, no. 2, pp. 297–311, Mar. 1988.

[36] M. Owe, R. de Jeu, and J. Walker, "A methodology for surface soil moisture and vegetation optical depth retrieval using the microwave polarization difference index," *IEEE Trans. Geosci. Remote Sens.*, vol. 39, no. 8, pp. 1643–1654, Aug. 2001.

[37] P. Hoekstra and A. Delaney, "Dielectric properties of soils at UHF and microwave frequencies," *J. Geophys. Res.*, vol. 79, no. 11, pp. 1699–1708, Apr. 1974.

[38] N. Wagner, K. Emmerich, F. Bonitz, and K. Kupfer, "Experimental investigations on the Frequency- and temperature-dependent dielectric material properties of soil," *IEEE Trans. Geosci. Remote Sens.*, vol. 49, no. 7, pp. 2518–2530, Jul. 2011.

[39] C. Park *et al.*, "A dielectric mixing model accounting for soil organic matter," *Vadose Zone J.*, vol. 18, no. 1, Jan. 2019, Art. no. 190036.

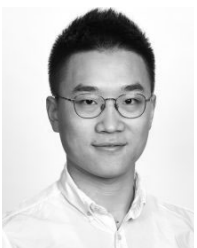

Xiaoji Shen (Graduate Student Member, IEEE) received the B.S. degree in geography information science and the M.Sc. degree in geography from Hohai University, Nanjing, China, in 2014 and 2017, respectively. He is pursuing the Ph.D. degree in civil engineering with Monash University, Clayton, VIC, Australia. His Ph.D. thesis aims at developing a model for P-band radiometer observations to achieve the soil moisture retrieval at P-band.

His research interests include passive microwave radiometry and microwave remote sensing of soil moisture.

Jeffrey P. Walker (Fellow, IEEE) received the B.E. degree in civil engineering, the Bachelor of Surveying degree (Hons.), and the Ph.D. degree in water resources engineering from The University of Newcastle, Callaghan, NSW, Australia, in 1995, 1995, and 1999, respectively.

He joined the National Aeronautics and Space Administration (NASA) Goddard Space Flight Centre, Greenbelt, MD, USA, in 1999, to implement his soil moisture (SM) work globally. In 2001, he joined the Department of Civil and Environmental Engineering, University of Melbourne, Melbourne, VIC, Australia, as a Lecturer. Since 2010, he has been a Professor with the Department of Civil Engineering, Monash University, Clayton, VIC, where he is continuing his research. He is contributing to SM satellite missions at NASA, European Space Agency (ESA), and JAXA, as a Science Team Member for the Soil Moisture Active Passive Mission and a Cal/Val Team Member for the Soil Moisture and Ocean Salinity and Global Change Observation Mission—Water, respectively.

Dr. Walker received the University Medal for Bachelor of Surveying from The University of Newcastle.

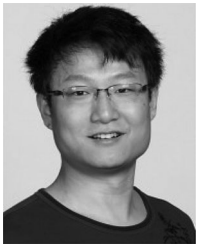

Nan Ye received the B.E. degree in hydraulic and hydropower engineering from Tsinghua University, Beijing, China, in 2006, and the Ph.D. degree in civil engineering from Monash University, Clayton, VIC, Australia, in 2014.

He coordinated a number of airborne field experiments for the in-orbit calibration/validation of the Soil Moisture Active Passive Mission in the Murrumbidgee River catchment, Southeast of Australia. He is a Senior Research Fellow with Monash University, working on P-band passive microwave remote sensing of soil moisture.

Xiaoling Wu (Member, IEEE) received the B.E. degree in biomedical engineering from Zhejiang University, Hangzhou, China, in 2009, and the Ph.D. degree in civil engineering from Monash University, Clayton, VIC, Australia, in 2015. Her undergraduate thesis was the development of biosensor using nanomaterial.

She was a Visiting Scholar with the Department of Computer Science, University of Copenhagen, Copenhagen, Denmark, from 2009 to 2010. The topic of her Ph.D. research was downscaling of soil moisture (SM) using airborne radar and radiometer observations in order to provide an accurate and high-resolution (better than 10 km) SM product with potential benefit in the areas of weather forecasting, flood, drought prediction, and agricultural activities. She is the Research Fellow with Monash University and continuing high-resolution SM work. Her research interests include microwave remote sensing of SM, SM downscaling, and proximal SM sensing for real-time agricultural applications.

Nithyapriya Boopathi (Graduate Student Member, IEEE) received the B.E. degree in civil engineering from the PSG College of Technology (Anna University), Coimbatore, India, in 2014, and the M.Tech. degree in remote sensing and GIS from the National Institute of Technology Karnataka Surathkal, Mangalore, India, in 2016. She is pursuing the Ph.D. degree in civil engineering with Monash University, Clayton, VIC, Australia, and the Center of Studies in Resources Engineering (CSRE), IIT Bombay, Mumbai, India, under the joint program by IITB-Monash Research Academy, Mumbai.

Her research focuses on ground-based P-band radiometer observations to analyze the feasibility of P-band in retrieving deeper soil moisture by exploring effective temperature and vegetation models. Her research interests include passive microwave remote sensing of soil moisture and aircraft-based radiometer studies.

In-Young Yeo received the B.S. degree in civil and environmental engineering from Seattle University, Seattle, WA, USA, in 1997, the M.Sc. degree in civil and environmental engineering and geodetic science and the Ph.D. degree in environmental planning both from the School of Engineering, The Ohio State University, Columbus, OH, USA, in 1999 and 2005, respectively.

She was a Faculty Member with the University of Maryland, College Park, MD, USA, Cornell University, Ithaca, NY, USA, and The Ohio State University, and a Graduate Research Fellow with the National Oceanic and Atmospheric Administration (NOAA) National Estuarine Research Reserve Systems, MD. She is an Associate Professor of Civil, Surveying, and Environmental Engineering with The University of Newcastle, Callaghan, NSW, Australia. She specializes in water resources engineering, geospatial engineering and environmental remote sensing, spatial optimization, and environmental planning. She has contributed to improving the monitoring and assessment of wetlands and soil hydrology, conservation management and practices for enhanced ecosystem services from agroecosystems, and developing tools and data for better decision support toward optimal land and water resources management at the catchment scale.

Linlin Zhang received the B.E. degree in surveying and mapping engineering from Central South University, Changsha, China, in 2015, and the Ph.D. degree in cartography and geography information system from the Aerospace Information Research Institute, Chinese Academy of Sciences, Beijing, China, in 2020.

From 2019 to 2020, she was a Visiting Ph.D. Student with Monash University, Clayton, VIC, Australia. The topic of her Ph.D. research was soil moisture retrieval from Gaofen-3 Synthetic Aperture Radar (SAR) satellite multipolarization observations. She is an Assistant Research Fellow with the Aerospace Information Research Institute, Chinese Academy of Sciences. Her research interests include active microwave remote sensing of soil moisture and multiangular soil moisture retrieval from L- and P-bands.

Liujun Zhu received the B.S. degree in geography from Zhejiang Normal University, Jinhua, China, in 2012, the M.Sc. degree in geography information science from Nanjing University, Nanjing, China, in 2015, and the Ph.D. degree in civil engineering from Monash University, Clayton, VIC, Australia, in 2019.

From 2017 to 2018, he was a Visiting Ph.D. Student with the University of Michigan, Ann Arbor, MI, USA. Since 2020, he has been an Adjunct Research Fellow with Monash University. His research interests include active microwave remote sensing, soil moisture retrieval, machine learning, and its applications in classification and change detection.